CrossMark

Effect of driver's anticipation in a new two-lane lattice model with the consideration of optimal current difference

Sapna Sharma

Abstract In this paper, a new lattice hydrodynamic traffic flow model is proposed by considering the driver's anticipation effect (DAE) in sensing optimal current difference (OCD) for two-lane system. The effect of anticipation parameter on the stability of traffic flow is examined through linear stability analysis and shown that it can significantly enlarge the stability region on the phase diagram. Nonlinear analysis is conducted, and mKdV equation is derived to describe propagation behavior of a density wave near the critical point. The driver's physical delay in sensing optimal current difference effect is also investigated and found that it has different effect on two-lane traffic based on whether lane changing is allowed or not. Simulation results are found in good agreement with the theoretical findings, which confirms that traffic jam can be suppressed efficiently by considering the DAEOCD effect in a two-lane traffic system.

S. Sharma (✉)
School of Mathematical Sciences, University of Science and Technology of China, Hefei 230026, China
e-mail: sapna2002@gmail.com

S. Sharma
Department of Mathematics, DAV University, Jalandhar 144001, India

1 Introduction

Due to the rapid increase in automobile on roads, the traffic problems became more and more serious and attracted much attention of scientists and researchers because of its complex mechanism, recently. Therefore, to understand the dynamics of traffic flow and investigate the properties of traffic jams, a considerable variety of traffic models have been developed and discussed by physicists, mathematicians, and so on [1–23] in past few decades. To explain the dynamical phase transitions on freeway, Nagatani [11] firstly in 1998 proposed a simple lattice hydrodynamic model and derived modified Korteweg–de Vries (mKdV) equation to describe the traffic congestion in terms of kink density wave near the critical point. Thereafter, this modeling approach was widely referred and extended to study various nonlinear phenomenon present in real traffic flow like backward effect [12], lateral effect of the lane width [13] and anticipation effect of potential lane changing [14]. Recently, Peng [15] incorporated the effect of anticipation individual driving behavior and proposed a new lattice model. Kang and Sun [16] introduced a lattice hydrodynamic model by taking into account driver's delay effect in sensing relative flux (DDSRF) and found that this effect has an important influence on the traffic jams.

Most of the aforementioned models focus mainly on some traffic phenomena only on a single lane. These models cannot fully describe the real traffic on roadways consists of two or more lanes since they do not consider the lane-changing behavior. In view of the above mentioned facts, Nagatani [24] further extended his model to two-lane system, two-dimensional traffic system [25] and also to high-dimensional [26] traffic dynamics. Later, some modifications have been made in two-lane lattice model by incorporating different factors like optimal current difference [27] and flow difference effect [28]. Peng [29] analyzed the effect of driver anticipation in two-lane system. Very recently, Gupta and Redhu [30] developed a new model to investigate the effect of driver's anticipation in sensing relative flux (DAESRF) for two-lane system.

In real traffic, the driver always adjusts his/her velocity according to observed traffic situation in the surroundings and estimates his/her driving individual behavior. Most of highways comprise of multi-lanes, so it will be more adequate to investigate this effect on a two-lane system with the consideration of potential lane changing. However, in the existing lattice models, driver's anticipation effect in sensing optimal current difference effect (DAEOCD) in two-lane system has not been studied. This motivates us to develop a two-lane lattice model by incorporating the effect of driver's anticipation individual behavior in sensing OCD effect.

In this paper, a more realistic lattice model with DAE in sensing OCD effect for two-lane traffic system is presented. In Sect. 3, the stability condition of traffic flow is investigated by means of linear stability theory. To describe the propagation behavior of traffic jams, Sect. 4 is devoted to the nonlinear analysis in which mKdV equation is derived near the critical point. Numerical simulations are carried out to validate the theoretical findings in Sect. 5, and finally, conclusions are drawn in Sect. 6.

2 A new model

To describe the traffic phenomena on single lane, the simplest lattice hydrodynamic model was, firstly, proposed by Nagatani [11] in 1998 and is given as

$$\partial_t \rho_j + \rho_0(\rho_j v_j - \rho_{j-1} v_{j-1}) = 0, \tag{1}$$

$$\partial_t(\rho_j v_j) = a[\rho_0 V(\rho_{j+1}) - \rho_j v_j]. \tag{2}$$

where ρ_0 is the average density; ρ_j and v_j, respectively, represent the local density and velocity at site j at time t. $V(.)$ is the optimal velocity function, which is a monotonically decreasing function having an upper bound and an inflection point at critical density. The idea is that the variation in traffic flow ρv at site j is determined by the difference between the actual flow at site j and the optimal flow $\rho_0 V(\rho_{j+1})$ at the next site.

While describing the traffic flow on road networks, multi-lane models are found to be more appropriate as most of the road networks are made up of more than one lane. In this regard, Nagatani [11] further extended single-lane lattice model to describe traffic phenomenon on two lanes by incorporating lane change effect in the lattice version of continuity equation. The lane changing on a two-lane highway occurs only in the following two cases.

Case (a): If $\rho_{2,j-1}(t) > \rho_{1,j}(t)$, i.e., the density at site $j - 1$ on the second lane is higher than that at site j on the first lane, the lane changing occurs from the second lane to the first lane and the lane-changing rate will be proportional to their density difference as follows: $\gamma|\rho_0^2 V'(\rho_0)| (\rho_{2,j-1}(t) - \rho_{1,j}(t))$.

Case (b): If $\rho_{1,j}(t) > \rho_{2,j+1}(t)$, i.e., the density at site j on the first lane is higher than that at site $j + 1$ on the second lane, the lane changing occurs from the first lane to the second lane and the lane-changing rate will be proportional to their density difference as follows: $\gamma|\rho_0^2 V'(\rho_0)| (\rho_{1,j}(t) - \rho_{2,j+1}(t))$.

Here, $\rho_{1,j}(t)$ and $\rho_{2,j}(t)$ are the densities on the first and second lane, respectively, and γ is a fixed dimensionless coefficient. The proportionality constant $(\gamma|\rho_0^2 V'(\rho_0)|)$ is chosen in such a way that it becomes dimensionless. Based on the above lane-changing rules, the continuity equation for two-lane traffic can be obtained in the same fashion as in Ref. [24] and is given by

$$\partial_t \rho_j + \rho_0(\rho_j v_j - \rho_{j-1} v_{j-1})$$
$$= \gamma|\rho_0^2 V'(\rho_0)|(\rho_{j+1} - 2\rho_j + \rho_{j-1}), \tag{3}$$

where $\rho_j = \frac{\rho_{1,j} + \rho_{2,j}}{2}$ represents the local density at site j and $\rho_j v_j = \frac{\rho_{1,j} v_{1,j} + \rho_{2,j} v_{2,j}}{2}$ represents the local flow at site j for the two-lane system.

In addition, the evolution equation of traffic current on each lane will not be affected by lane changing. Hence, the evolution equation for two-lane traffic [24] was incorporated as

$$\partial_t(\rho_j v_j) = a[\rho_0 V(\rho_{j+1}) - \rho_j v_j]. \tag{4}$$

Further, Peng [27] extended the Nagatani's two-lane lattice model by considering the optimal current difference effect and found that it has an important influence on multi-lane traffic flow system. The continuity equation remains preserved, while the evolution equation is modified by looking at the difference of optimal traffic currents on site—$j + 2$ and $j + 1$. This effect plays a significant role in stabilizing the traffic flow and suppresses effectively the traffic jams. Then, the modified evolution equation is given by

$$\partial_t(\rho_j v_j) = a\rho_0 V(\rho_{j+1}) - a\rho_j v_j$$
$$+ a\lambda[\rho_0 V(\rho_{j+2}) - \rho_0 V(\rho_{j+1})]. \tag{5}$$

Here, λ is the reaction coefficient of optimal current difference. However, the important aspect of driver's anticipation effect (DAE) was not incorporated in this lattice traffic flow model. As observed in real traffic flow, drivers always adjust their vehicles based on the available dynamic estimation information. In this dynamic process, drivers sense the traffic relative information from surroundings at time t and make a decision to adjust velocity of their vehicles at a later time $t + \tau_1$, where τ_1 is the delay of driver's response in sensing headway. Once the decision has been taken, vehicle actually moves at some later time $t + \tau_1 + \tau_2$ due to the delay of car motion, where τ_2 represents the delay time of car motion. So, the total delay time is the sum of two different delay times τ_1 and τ_2. Without lose of generality, a linear relationship between driver's response delay τ_1 and the total delay time τ is chosen as $\tau_1 = \alpha\tau$, where the α is the anticipation coefficient that corresponds to driver's behavior and $\tau = 1/a$ denote the delay time, which allows for the time lag, that it takes the traffic current to reach the optimal current when the traffic is varying. However, driver's anticipation effect was not explicitly considered in two-lane Peng's model [27]. Therefore, we propose a new evolution equation with consideration of anticipation driving effect in sensing optimal current difference effect (DAEOCD) on a two-lane system as follows:

$$\partial_t(\rho_j(t)v_j(t)) = a\rho_0 V[\rho_{j+1}(t + \alpha\tau)] - a\rho_j(t)v_j(t)$$
$$+ a\lambda[Q_{j+2}(t+\alpha\tau) - Q_{j+1}(t+\alpha\tau)]. \tag{6}$$

where $Q_j(t) = \rho_0 V[\rho_j(t)]$ and the last term in the above evolution equation denote the optimal current difference on site $j + 1$. In the proposed model, the sign of anticipation coefficient α explores different characteristics of driver's behavior on two-lane highway. The positive value of α represents anticipation driving behavior or the drivers forecast effect in a traffic system with intelligent transportation system (ITS). Here, driver adjusts his driving individual speed to the anticipation optimal speed at time $t + \alpha\tau$ after delay time τ in advance. So, the bigger value of α corresponds to more skillful drivers in the model.

For $\alpha < 0$, i.e., negative anticipation coefficient corresponds to the explicit driver's physical delay in sensing optimal current difference effect. The effect of driver's delay in sensing relative flux is also analyzed in single-lane model by Kang and Sun [16] and for two-lane traffic system by Zhang et al. [31], recently. When $\alpha = 0$, the new model reduces to Peng's [27]. For simplicity, using the Taylor series expansion and neglecting the nonlinear terms, the new evolution equation can be obtained as:

$$\partial_t(\rho_j(t)v_j(t)) = a\rho_0[V(\rho_{j+1}(t))$$
$$+ \alpha\tau V'(\rho_{j+1}(t))\partial_t\rho_{j+1}(t)] - a\rho_j(t)v_j(t)$$
$$+ a\lambda\rho_0[V(\rho_{j+2}(t)) - V(\rho_{j+1}(t))]$$
$$+ a\lambda\alpha\tau\rho_0[V'(\rho_{j+2}(t))\partial_t\rho_{j+2}(t)$$
$$- V'(\rho_{j+1}(t))\partial_t\rho_{j+1}(t)]. \tag{7}$$

By taking the difference form of Eqs. (3) and (7) and eliminating speed v_j, the density equation is obtained as

$$\rho_j(t + 2\tau) - \rho_j(t + \tau) + \tau\rho_0^2[V(\rho_{j+1}(t))$$
$$- V(\rho_j(t))]$$
$$+ \alpha\rho_0^2\tau[V'(\rho_{j+1}(t))\tilde{\Delta}\rho_{j+1}(t) - V'(\rho_j(t))\tilde{\Delta}\rho_j(t)]$$
$$+ \lambda\tau\rho_0^2[V(\rho_{j+2}(t)) - 2V(\rho_{j+1}(t)) + V(\rho_j(t))]$$
$$+ \alpha\tau\lambda\rho_0^2[V'(\rho_{j+2}(t))\tilde{\Delta}\rho_{j+2}(t)$$
$$- 2V'(\rho_{j+1}(t))\tilde{\Delta}\rho_{j+1}(t) + V'(\rho_j(t))\tilde{\Delta}\rho_j(t)]$$
$$- \tau\gamma|\rho_0^2 V'(\rho_0)|[\rho_{j+1}(t + \tau)$$
$$- 2\rho_j(t + \tau) + \rho_{j-1}(t + \tau)] = 0, \tag{8}$$

where $\tilde{\Delta}\rho_j(t) = \rho_j(t + \tau) - \rho_j(t)$.

3 Linear stability analysis

To investigate the influence of driver anticipation effect on jamming transition of traffic flow, linear stability

analysis is conducted on the extended model in this section. For this, under the condition of homogeneous traffic flow, the state of uniform traffic is defined by constant density ρ_0 and optimal velocity $V(\rho_0)$. Hence, the steady-state solution of the homogeneous traffic flow is given as

$$\rho_j(t) = \rho_0, \quad v_j(t) = V(\rho_0). \tag{9}$$

Let $y_j(t)$ be a small deviation to the steady-state density on site j. Then,

$$\rho_j(t) = \rho_0 + y_j(t). \tag{10}$$

Putting this perturbed density profile into Eq. (8) and linearizing it, we obtain

$$
\begin{aligned}
&y_j(t + 2\tau) - y_j(t + \tau) + \tau\rho_0^2 V'(\rho_0)[y_{j+1}(t) - y_j(t)] \\
&\quad + \alpha\tau\rho_0^2 V'(\rho_0)\tilde{\Delta}[y_{j+1}(t) - y_j(t)] \\
&\quad + \lambda\rho_0\tau V'(\rho_0)[y_{j+2}(t) - 2y_{j+1}(t) + y_j(t)] \\
&\quad + \alpha\tau\lambda\rho_0^2 V'(\rho_0)\tilde{\Delta}[y_{j+2}(t) - 2y_{j+1}(t) + y_j(t)] \\
&\quad - \tau\gamma|\rho_0^2 V'(\rho_0)|[y_{j+1}(t + \tau) - 2y_j(t + \tau) \\
&\quad + y_{j-1}(t + \tau)] = 0.
\end{aligned}
\tag{11}
$$

Substituting $y_j(t) = exp(ikj + zt)$ in Eq. (11), we get

$$
\begin{aligned}
&e^{2\tau z} - e^{\tau z} + \tau\rho_0^2 V'(\rho_0)[e^{ik} - 1] \\
&\quad + \alpha\tau\rho_0^2 V'[e^{\tau z} - 1][e^{ik} - 1] \\
&\quad + \lambda\rho_0^2\tau V'(\rho_0)[e^{ik} - 1]^2 \\
&\quad + \lambda\tau\rho_0^2\alpha V'(\rho_0)[e^{\tau z} - 1][e^{ik} - 1]^2 \\
&\quad - \tau\gamma|\rho_0^2 V'(\rho_0)|[e^{ik} - 2 + e^{-ik}]e^{\tau z} = 0.
\end{aligned}
\tag{12}
$$

Inserting $z = z_1(ik) + z_2(ik)^2 \ldots$ into Eq. (12), we obtained the first-order and second-order terms of the coefficient ik and $(ik)^2$, respectively, as

$$z_1 = -\rho_0^2 V'(\rho_0), \tag{13}$$

$$
z_2 = -\frac{3\tau z_1^2}{2} - \frac{\rho_0^2 V'(\rho_0)}{2} - \tau\alpha\rho_0^2 V'(\rho_0)z_1 \\
\quad - \lambda\rho_0^2 V'(\rho_0) + \gamma|\rho_0^2 V'(\rho_0)|.
\tag{14}
$$

When $z_2 < 0$, the uniform steady-state flow becomes unstable for long-wavelength waves. For $z_2 > 0$, the uniform flow becomes stable. Thus, the stability condition for the steady state is

$$\tau = -\frac{1 + 2\gamma + 2\lambda}{\rho_0^2 V'(\rho_0)(3 - 2\alpha)}. \tag{15}$$

The instability condition for the homogeneous traffic flow can be described as

$$\tau > -\frac{1 + 2\gamma + 2\lambda}{\rho_0^2 V'(\rho_0)(3 - 2\alpha)}. \tag{16}$$

As $\alpha = 0$, the above unstability criteria (Eq. 16) will become same as that of Peng's model [27].

Eq. (16) clearly shows that lane-changing parameter γ, anticipation coefficient α and reaction coefficient λ play a significant role on the stability of traffic flow. The neutral stability curves in the phase space (ρ, a) are shown by solid curves in Fig. 1 for different values of α. Figure 1a corresponds to without lane changing, i.e., $\gamma = 0$ and Fig. 1b corresponds the lane-changing case for $\gamma = 0.1$. It can be observed from the figures that the apex of these curves (ρ_c, a_c) decreases with an increase in α in both the cases, which means that larger value of α leads to enlargement of stability region, and hence, the traffic jam is suppressed efficiently. For negative values of α, when explicit driver's physical delay is present, the instability region increases, which is in accordance with the result of Gupta and Redhu [30] for two-lane and Kang and Sun [16] for single-lane traffic models. On comparing Fig. 1a, b, it can also be concluded that under the same conditions, the traffic flow has been strengthen with the increase in the value of γ, which means that lane changing reduces traffic jams significantly. This is similar to the real traffic phenomenon as under the jam situation, vehicles try to accommodate themselves in a less denser lane by changing their lane quite frequently to overcome the congestion.

4 Nonlinear stability analysis

In this section, we investigate the evolution characteristic of traffic jam around the critical point (ρ_c, a_c) on coarse-grained scales using reduction perturbation technique. Long-wavelength expansion method is used to understand the slowly varying behavior near the critical point. For that, the slow variables X and T for a small positive scaling parameter $\epsilon(0 < \epsilon \ll 1)$ are defined as follows:

$$X = \epsilon(j + bt), \quad T = \epsilon^3 t, \tag{17}$$

where b is a constant to be determined. Let ρ_j satisfy the following equation:

$$\rho_j(t) = \rho_c + \epsilon R(X, T). \tag{18}$$

By expanding Eq. (8) using Taylor expansion up to fifth order (see Appendix 1) of ϵ with the help of Eqs. (17) and (18), the following nonlinear equation is obtained.
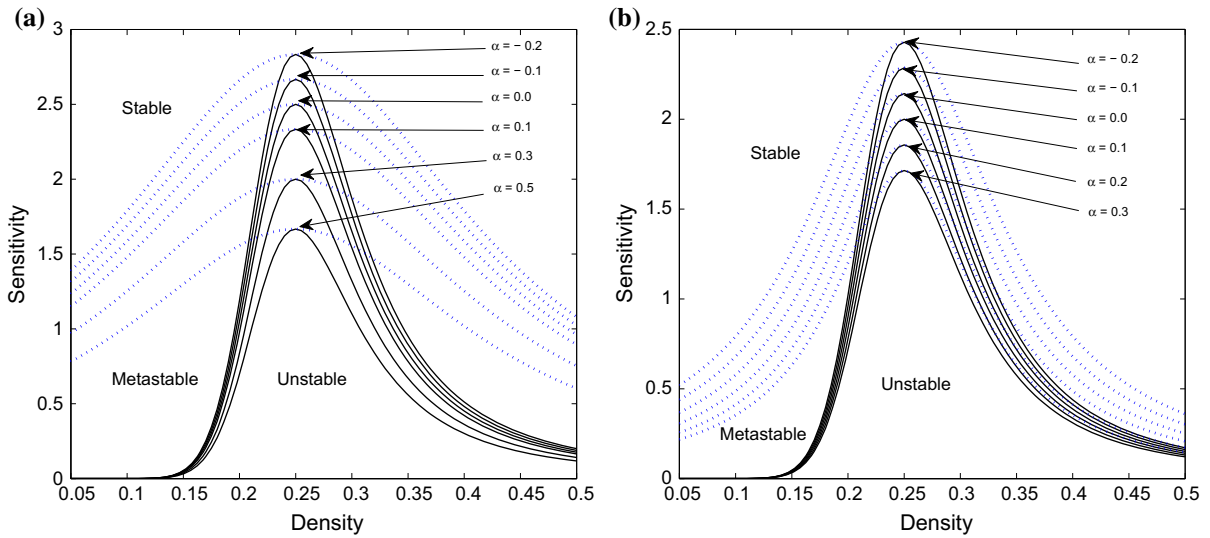
Fig. 1 Phase diagram in parameter space (ρ, a), $\lambda = 0.1$ for **a** $\gamma = 0$, and **b** $\gamma = 0.1$, respectively

Table 1 The coefficients k_i of the model

k_1	k_2	k_3	
$b + \rho_c^2 V'$	$\frac{3}{2}b^2\tau + \rho_c^2 V'\left[\frac{1}{2} + b\alpha\tau + \lambda + \gamma\right)]$	$\frac{7}{6}b^3\tau^2 + \frac{\rho_c^2 V'}{6}\left[1 + 3\alpha b\tau(1+b\tau) + 6\lambda + 6\alpha b\tau\lambda + 6\gamma b\tau\right]$	
k_4	k_5	k_6	k_7
$\frac{\rho_c^2 V'''}{6}$	$3b\tau + \alpha\tau\rho_c^2 V'$	$\frac{5}{8}b^4\tau^3 + \frac{\rho_c^2 V'}{6}\left[\frac{1}{4} + \frac{7\lambda}{2} + \alpha\left(b\tau + \frac{3b^2\tau^2}{2} + b^3\tau^3\right)\right.$ $\left. +3\alpha\lambda[b^2\tau^2 + 2b\tau] + \frac{\gamma(1+6b^2\tau^2)}{2}\right]$	$\frac{(2\lambda-1)\rho_c^2 V'''}{12}$

$$\epsilon^2 k_1 \partial_X R + \epsilon^3 k_2 \partial_X^2 R$$
$$+ \epsilon^4 (\partial_T R + k_3 \partial_X^3 R + k_4 \partial_X R^3)$$
$$+ \epsilon^5 (k_5 \partial_T \partial_X R + k_6 \partial_X^4 R + k_7 \partial_X^2 R^3) = 0. \quad (19)$$

The coefficients k_i $(i = 1, 2, \cdots, 7)$ are given in Table 1, where $V' = \frac{dV(\rho)}{d\rho}|_{\rho=\rho_c}$, $V''' = \frac{dV^3(\rho)}{d\rho^3}|_{\rho=\rho_c}$. Near the critical point (ρ_c, a_c), the value of τ is set as

$$\tau = \tau_c(\epsilon^2 + 1). \quad (20)$$

By taking $b = -\rho_c^2 V'$ and eliminating the second-order and third-order terms of ϵ, we obtain

$$\epsilon^4(\partial_T R - g_1 \partial_X^3 R + g_2 \partial_X R^3)$$
$$+ \epsilon^5(g_3 \partial_X^2 R + g_4 \partial_X^4 R + g_5 \partial_X^2 R^3) = 0, \quad (21)$$

where the coefficients g_i $(1, 2, \cdots, 5)$ are shown in Table 2.

In order to determine the value of propagation velocity for the kink–antikink solution, it is necessary to satisfy the following condition:

$$(R_0', M[R_0']) \equiv \int_{-\infty}^{\infty} dX R_0' M[R_0'] = 0, \quad (22)$$

with $M[R_0'] = M[R']$. By solving Eq. (22), the selected value of c is

$$c = \frac{5g_2 g_3}{2g_2 g_4 - 3g_1 g_5}. \quad (23)$$

Hence, the kink–antikink solution is given by

$$\rho_j = \rho_c + \epsilon\sqrt{\frac{g_1 c}{g_2}} \tanh\left(\sqrt{\frac{c}{2}}(X - cg_1 T)\right), \quad (24)$$

with $\epsilon^2 = \frac{a_c}{a} - 1$ and the amplitude A of the solution is

Table 2 The coefficients g_i of the model

g_1	g_2	g_3
$-\frac{7}{6}b^3\tau_c^2 - \frac{\rho_c^2 V'}{6}[1 + 3\alpha b\tau_c(1 + b\tau_c)$ $+ 6\lambda + 6\alpha b\tau_c\lambda + 6\gamma b\tau_c]$	$\frac{\rho_c^2 V'''}{6}$	$\frac{3}{2}b^2\tau_c + b\alpha\tau_c\rho_c^2 V'$

g_4	g_5
$(3b + \alpha\rho_c^2 V')\tau_c g_1 + \frac{5}{8}b^4\tau_c^3 + \frac{\rho_c^2 V'}{6}\left[\frac{1}{4} + \frac{7\lambda}{2} + \frac{\gamma(1+6b^2\tau_c^2)}{2}\right.$ $\left. + 3\alpha\lambda[b^2\tau_c^2 + 2b\tau_c] + \alpha\left(b\tau_c + \frac{3b^2\tau_c^2}{2} + b^3\tau_c^3\right)\right]$	$\frac{(2\lambda-1)\rho_c^2 V'''}{12}$

$$A = \sqrt{\frac{g_1}{g_2}\epsilon^2 c}. \tag{25}$$

The kink–antikink soliton solution represents the coexisting phase including both freely moving phase (within low density) and congested phase (within high density), which can be described by $\rho_j = \rho_c \pm A$, respectively, in the phase space (ρ, a). For a particular case, when $\alpha = 0$, the results become similar to those found by Peng [27]. The dashed lines in Fig. 1 represent the coexisting curves, which divide the phase plane into three regions: the stable region, the metastable region and the unstable region. In the stable region, the traffic flow will remain stable under a disturbance, while in metastable and unstable region, a small disturbance will lead to the congested traffic. Moreover, with the consideration of DAE when lane changing is allowed, the corresponding neutral and coexisting curves both lower down, which means that the stability of uniform traffic flow has been further strengthen, while the negative
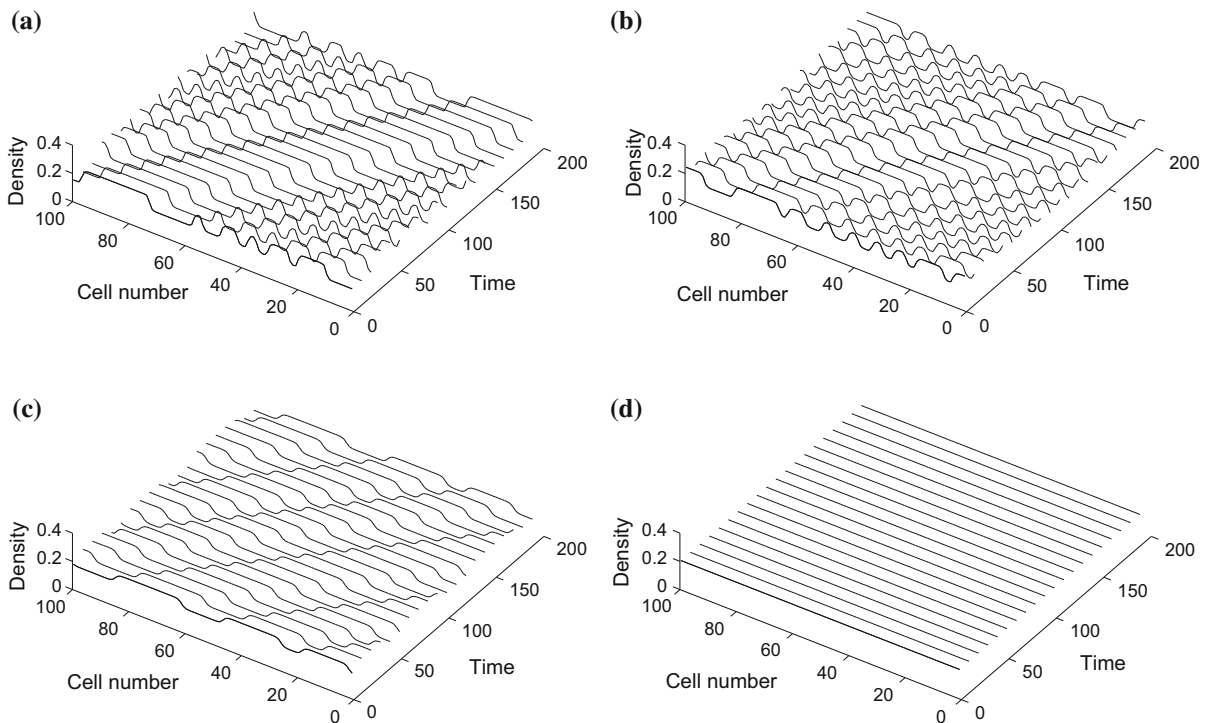

Fig. 2 Spatiotemporal evolutions of density when $\gamma = 0$, $\lambda = 0.1$ for **a** $\alpha = 0$, **b** $\alpha = 0.1$, **c** $\alpha = 0.3$, and **d** $\alpha = 0.5$, respectively
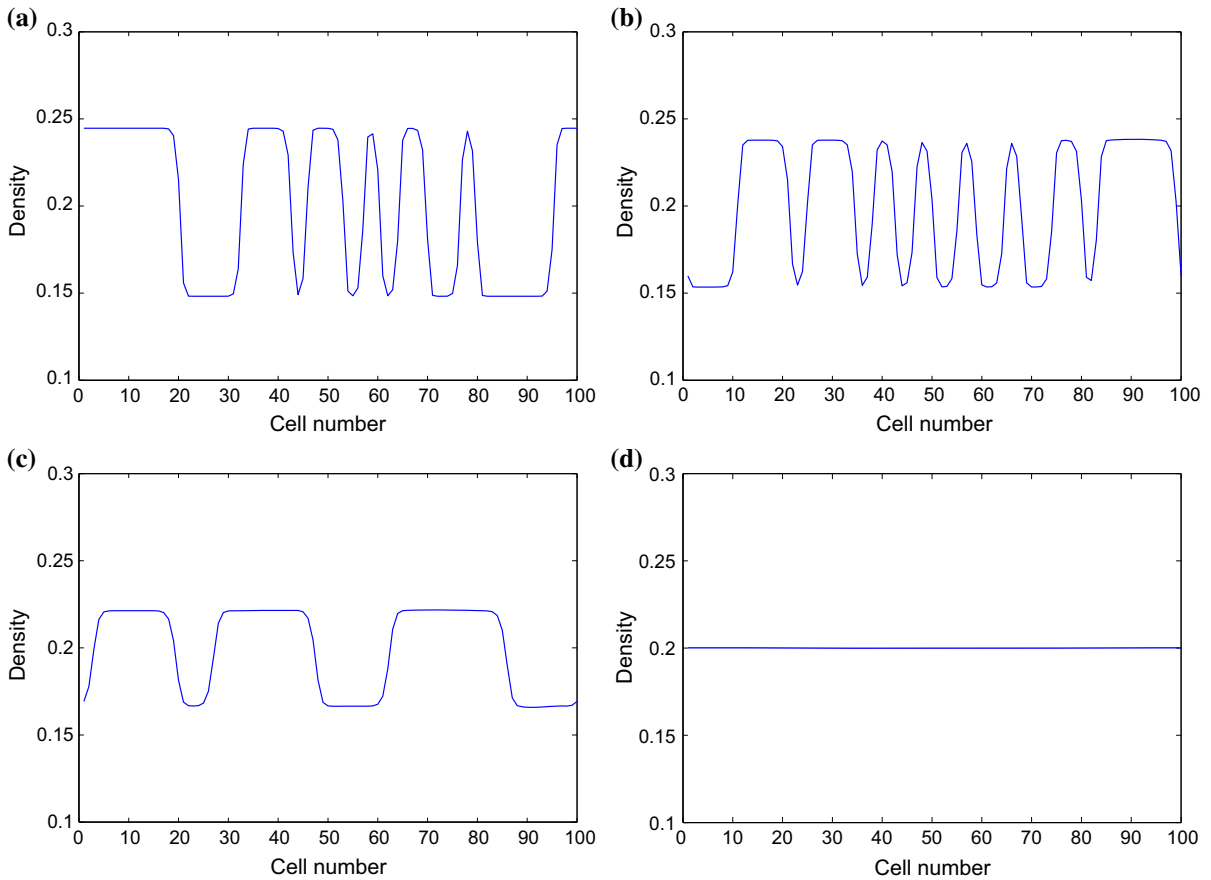
Fig. 3 Density profile at time $t = 20300$ when $\gamma = 0$, $\lambda = 0.1$ for **a** $\alpha = 0$, **b** $\alpha = 0.1$, **c** $\alpha = 0.3$, and **d** $\alpha = 0.5$, respectively

value of α produces the opposite effect and the amplitude of these curves increases, which leads to reduction in the stability region of traffic flow.

5 Numerical simulation

In this section, we carry out numerical simulation of the new model to investigate the effect of drivers anticipation on traffic flow dynamic as well as to validate linear and nonlinear analysis. Periodic boundary conditions are chosen, and the initial conditions are taken as follows:

$$\rho_j(1) = \rho_j(0) = \begin{cases} \rho_0; & j \neq \frac{M}{2}, \frac{M}{2}+1 \\ \rho_0 - \sigma; & j = \frac{M}{2} \\ \rho_0 + \sigma; & j = \frac{M}{2}+1 \end{cases}$$

where σ is the initial disturbance, M is the total number of sites taken as 100, and other parameters are set as follows: $\sigma = 0.1$, $a = 2.3$, $\tau = \frac{1}{a}$.

The optimal velocity function given by Nagatani [24] is adopted.

$$V(\rho) = \frac{V_{\max}}{2} \left[\tanh\left(\frac{1}{\rho} - \frac{1}{\rho_c}\right) + \tanh\left(\frac{1}{\rho_c}\right) \right], \quad (26)$$

where $V_{\max}$ and ρ_c denote the maximal velocity and the safety critical density, respectively. The optimal velocity function is monotonically decreasing and has an upper bound and a turning point at $\rho = \rho_c = \rho_0$. For computation, maximal velocity and critical density are set at 2.0 and 0.25, respectively.

Figure 2 depicts the simulation results of spatiotemporal evolution of density after 2×10^4 time steps for different values of α under no lane-changing situation ($\gamma = 0$) and $\lambda = 0.1$. It is clear from the Fig. 2a–d that initial disturbance leads to the kink–antikink soliton, which propagates in the backward direction. Due to this, initial uniform flow under a small amplitude

disturbance evolves into congested flow as the stability condition is not satisfied. Figure 2d shows that as soon as $\alpha = 0.4$, i.e., we entered into the stable region, a small amplitude perturbation to the homogeneous density dies out and stop-and-go wave disappears. It is also clear from Fig. 2a–d that anticipation driving behavior has efficiently suppressed the traffic jam and also validate the theoretical findings when lane changing is not allowed.

Figure 3 describes the density profile at time $t = 20, 300$ s corresponding to panel of Fig. 2. It can be easily depicted from Fig. 3a–d that the number of stop-and-go waves gradually decreases with an increase in anticipation coefficient. This validates the fact that in real traffic, more skillful drivers help in removing the traffic congestion. The region of free flow turns wide, and the amplitude of density waves is weakened with the increase in anticipation coefficient, which means that anticipation effect enhances the stability of the traffic flow. The traffic jam disappears, and flow becomes homogeneous at $\alpha = 0.5$. Therefore, it is worth to conclude that driver's anticipation effect significantly enhances the stability of system.

Now, we examined the effect of anticipation coefficient α on traffic flow dynamics when lane changing is allowed ($\gamma = 0.1$). Figures 4 and 5 display the simulation results under the different values of anticipation coefficient α for $\lambda = 0.1$. The results corresponding to $\gamma = 0.1$ are found qualitatively similar to those obtained for $\gamma = 0$. Parallel to no lane-changing case, initial small amplitude disturbance is amplified in patterns (a, c), while the disturbance will dissolve quickly and the traffic flow becomes uniform over the whole space for an appropriate value of the parameter α as shown in pattern (d). It is also clear from the density profile (Fig. 5d) that the traffic flow becomes stable for small value of anticipation coefficient for lane changing in comparison with without lane-changing situation. This verifies that more skillful drivers play a crucial role in avoiding jams when lane changing is permitted in two-lane system. It indicates that the stability of the new two-lane lattice model is better than that of Nagatani's lattice model by taking the DAE's effect into consideration.

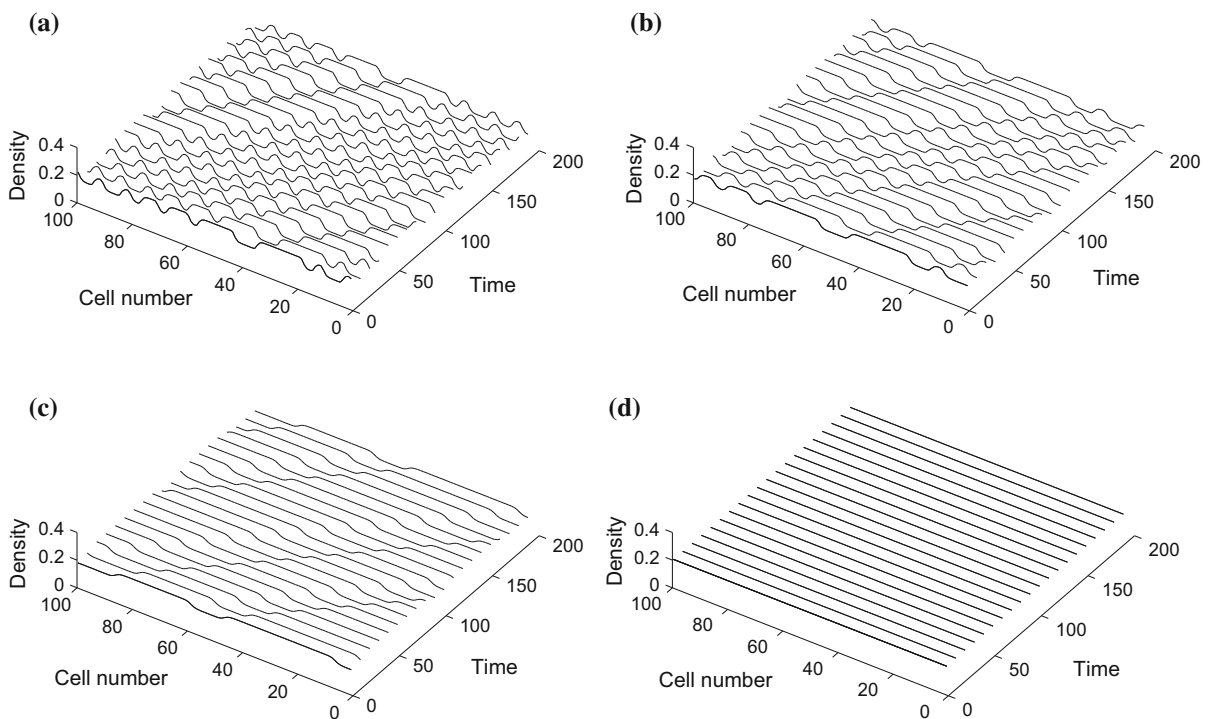We further investigate the effect of negative anticipation coefficient representing the explicit drier's phys-

Fig. 4 Spatiotemporal evolutions of density when $\gamma = 0.1$, $\lambda = 0.1$ for **a** $\alpha = 0$, **b** $\alpha = 0.1$, **c** $\alpha = 0.2$, and **d** $\alpha = 0.3$, respectively
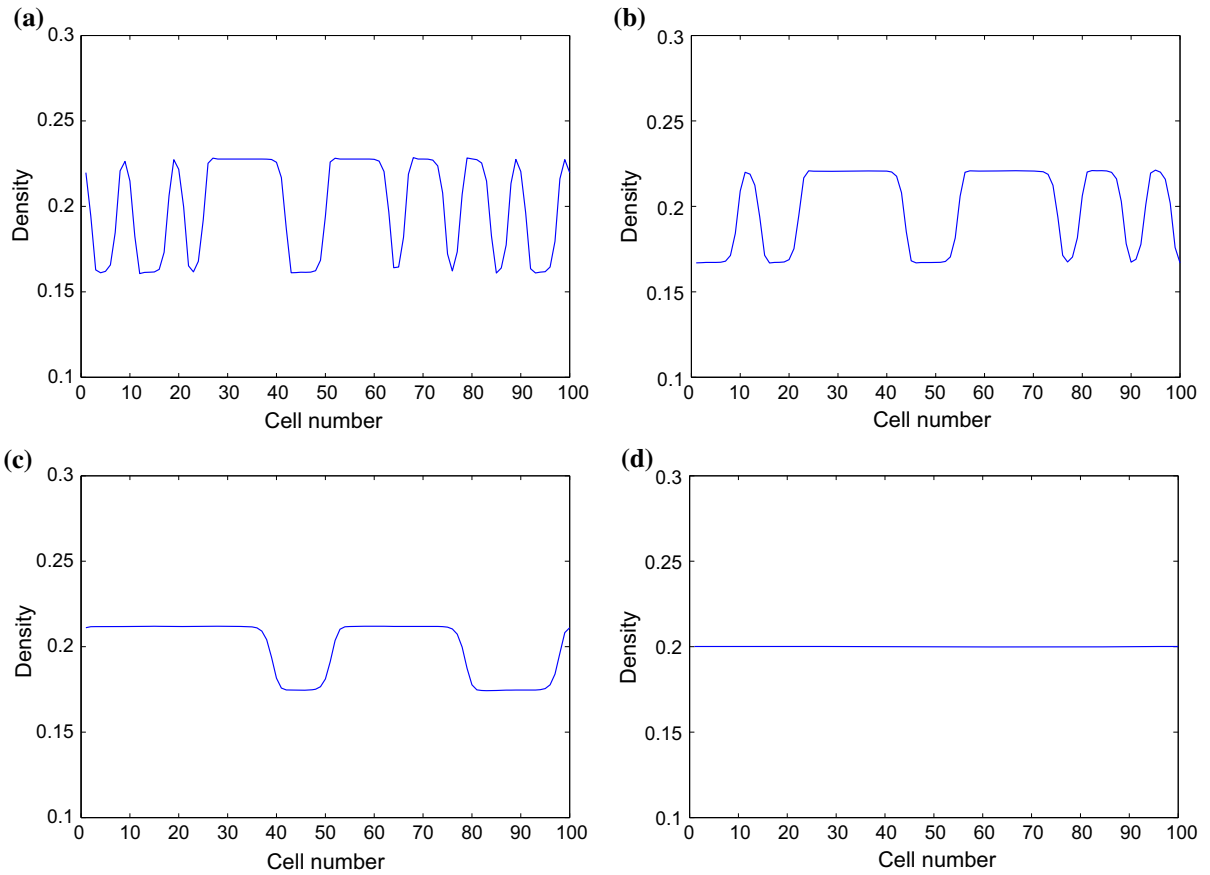
Fig. 5 Density profile at time $t = 20300$ when $\gamma = 0.1$, $\lambda = 0.1$ for **a** $\alpha = 0$, **b** $\alpha = 0.1$, **c** $\alpha = 0.2$, and **d** $\alpha = 0.3$, respectively
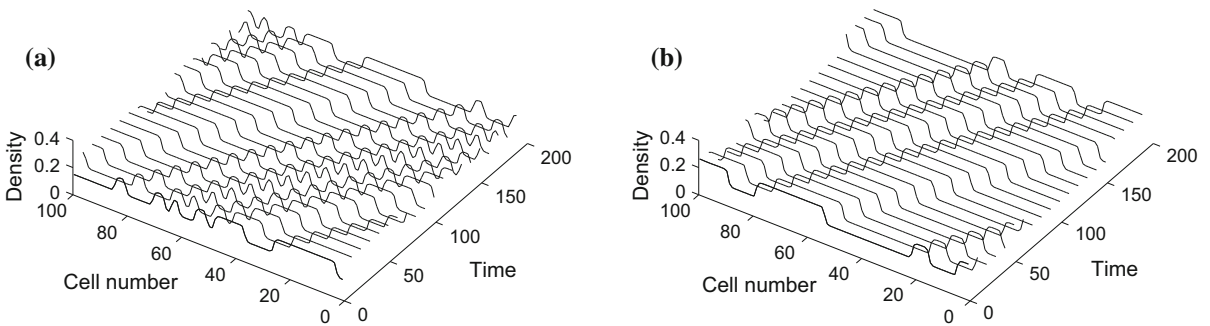

Fig. 6 Spatiotemporal evolutions of density when $\gamma = 0$, $\lambda = 0.1$ for **a** $\alpha = -0.1$, and **b** $\alpha = -0.2$, respectively

ical delay in sensing optimal current difference effect. Figures 6 and 7 show the simulation results when $\alpha < 0$ and lane changing are not allowed ($\gamma = 0.0$). It is clear from the Fig. 6a, b that driver's delay in sensing optimal current difference effect plays an important role in traffic congestion. The amplitude of the density waves

increases with an increase in the explicit drier's physical delay, which means that jam can easily appear as the driver has large delay of response.

Figures 8 and 9 show the simulation results when the anticipation coefficient takes the negative values and lane changing is permitted ($\gamma = 0.1$). The results
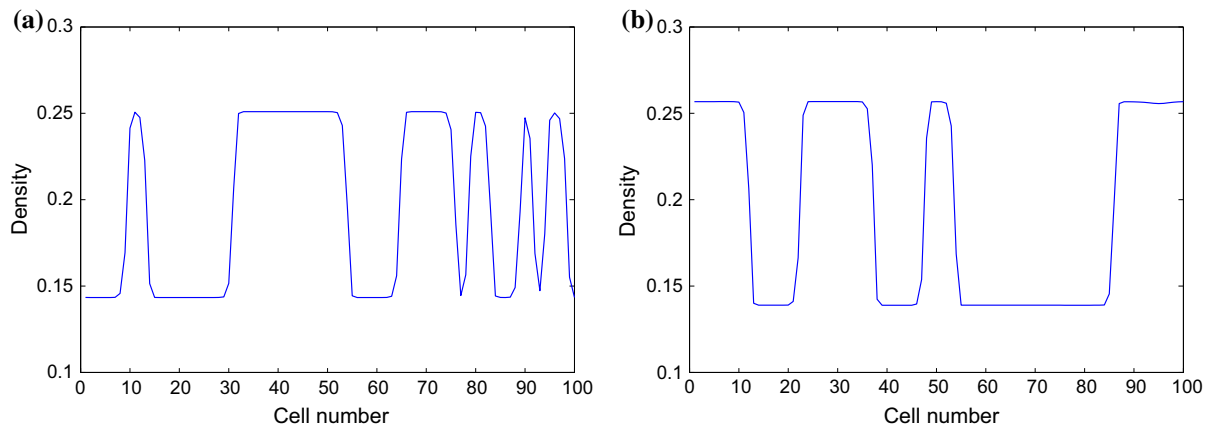
Fig. 7 Density profile at time $t = 10300$ when $\gamma = 0$, $\lambda = 0.1$ for **a** $\alpha = -0.1$, and **b** $\alpha = -0.2$, respectively
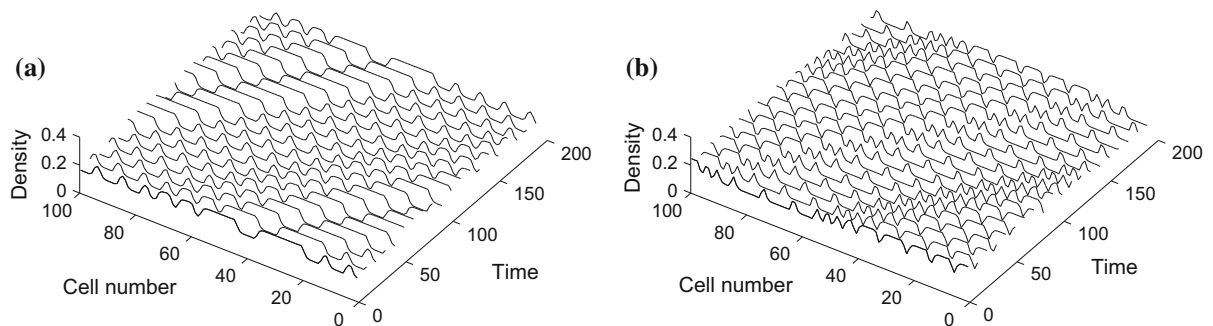

Fig. 8 Spatiotemporal evolutions of density when $\gamma = 0.1$, $\lambda = 0.1$ for **a** $\alpha = -0.1$, and **b** $\alpha = -0.2$, respectively

corresponding to $\gamma = 0.1$ are quite different from those obtained for $\gamma = 0$. On comparing Fig. 7 with Fig. 9, it is observed that the density profiles of congested flow in passing case are no longer periodic. This jam pattern exhibits irregular complex structure and propagates in the opposite direction to the vehicle's movement that is a characteristic of chaos. In chaotic flow, density waves band with one another, break up, and propagates in the backward direction. From these results, we can conclude that kink–antikink as well as chaotic region can exist in the instable region on the phase plane for different values of α when passing is allowed in two-lane traffic system.

Figures 10 and 11 represent the phase space plot of density difference $\rho(t) - \rho(t - 1)$ against $\rho(t)$ for $t = 10000 - 20000$ corresponding to the traffic flows in Figs. 7 and 9, respectively. Figure 10 of kink jam

exhibit the limit cycle, which corresponds to the periodic traffic behavior. The points on the right and left ends represent, respectively, the states within the traffic jams and within the freely moving phase. The pattern in Fig. 11 represents the set of dispersed points around a closed loop in the phase space plot. It corresponds to the irregular traffic behavior, which exhibits the behavior characteristic of chaos. It is also clear from the figure that the chaotic jam becomes more stronger by decreasing the vale of α, which validates the fact that as the driver's delay increases, the traffic becomes more and more irregular on a two-lane highway when lane changing is allowed. Therefore, from theoretical and simulation results, it is reasonable to conclude that traffic jam can efficiently be suppressed by incorporating the driver's anticipation effect on a two-lane traffic system.
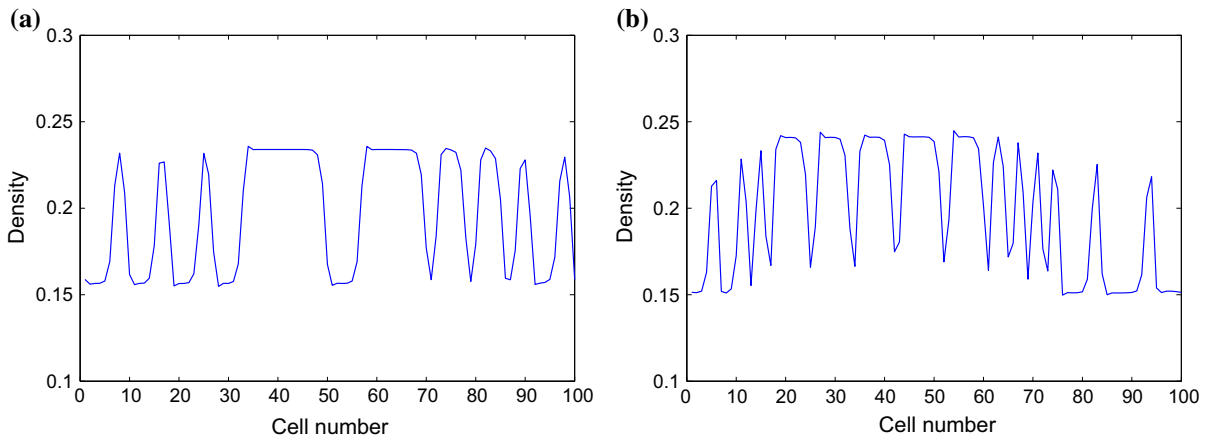
Fig. 9 Density profile at time $t = 10300$ when $\gamma = 0.1$, $\lambda = 0.1$ for **a** $\alpha = -0.1$, and **b** $\alpha = -0.2$, respectively
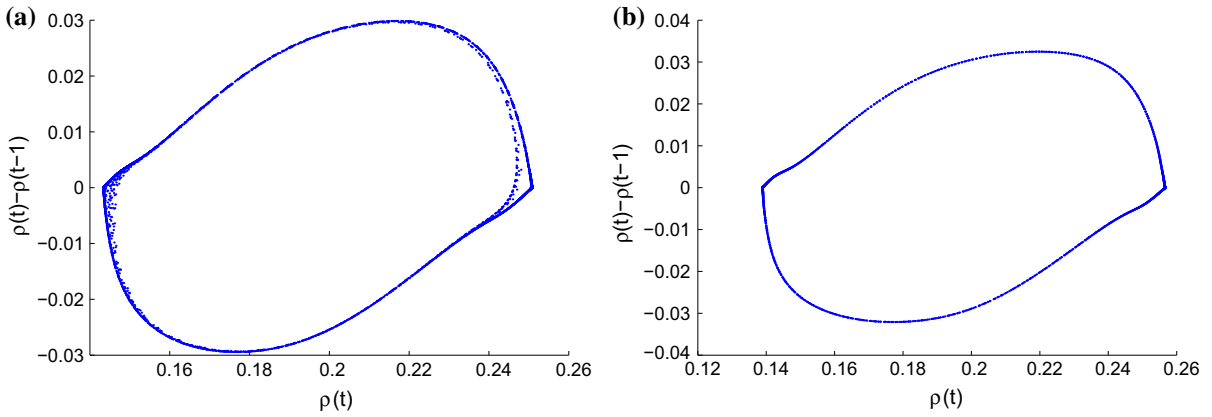

Fig. 10 Plot of density difference against density corresponds to the panels in Fig. 8, respectively
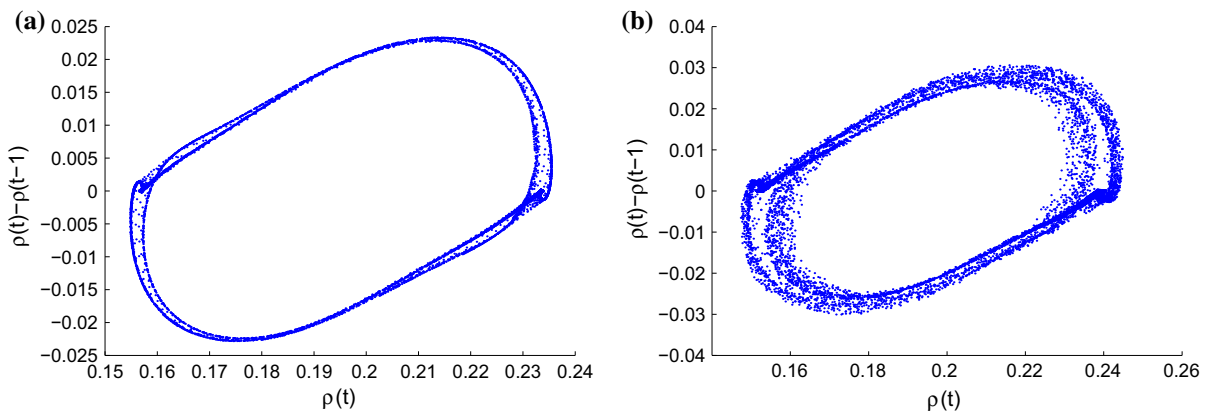

Fig. 11 Plot of density difference against density corresponds to the panels in Fig. 9, respectively

6 Conclusion

In this paper, we presented a new lattice hydrodynamic model for two-lane traffic flow by considering anticipation driving individual behavior in sensing optimal current difference effect (DAEOCD). Linear and nonlinear analyses are performed to investigate the traffic behavior analytically. We derived the mKdV equation to describe the traffic jam near the critical point and obtained kink–antikink soliton solution related to the traffic flow density. In addition, phase diagrams in the density-sensitivity space with the neutral stability curves and the coexisting curves are presented, showing the phase transition among the freely moving phase to uniform congested phase through coexisting phase in two-lane system. It is concluded that anticipation coefficient corresponds to driver's behavior in sensing that optimal current difference increases the stability of traffic flow significantly in two-lane system, while the negative value of anticipation coefficient corresponds to driver's delay response in sensing that optimal current difference effect reduces the stable region and increases congestion. The simulation results are in good accordance with the theoretical findings. Therefore, it is reasonable to conclude that driver's anticipation effect plays an important role in stabilizing/destabilizing the traffic flow on two-lane highway. Though the results discussed in this paper are complete, yet the proposed two-lane model will be analyzed in our future work to incorporate many important factors discussed in Refs. [1–10] .

Appendix 1

In this appendix, we give the expansion of each terms in Eq. (8) using Eqs. (17) and (18) to the fifth order of ϵ.

$$
\begin{aligned}
\rho_j(t+\tau) = \rho_c + \epsilon R + \epsilon^2(b\tau)\partial_X R \\
+ \frac{\epsilon^3}{2}(b\tau)^2\partial_X^2 R + \frac{\epsilon^4}{6}(b\tau)^3\partial_X^3 R + \epsilon^4\tau\partial_T R \\
+ \frac{\epsilon^5}{24}(b\tau)^4\partial_X^4 R + \epsilon^5 b\tau^2\partial_T\partial_X R.
\end{aligned}
\tag{27}
$$

$$
\begin{aligned}
\rho_j(t+2\tau) = \rho_c + \epsilon R + \epsilon^2(2b\tau)\partial_X R \\
+ \frac{\epsilon^3}{2}(2b\tau)^2\partial_X^2 R
\end{aligned}
$$

$$
\begin{aligned}
+ \frac{\epsilon^4}{6}(2b\tau)^3\partial_X^3 R + \epsilon^4(2\tau)\partial_T R \\
+ \frac{\epsilon^5}{24}(2b\tau)^4\partial_X^4 R + \epsilon^5(4b\tau^2)\partial_T\partial_X R.
\end{aligned}
\tag{28}
$$

$$
\begin{aligned}
\rho_{j+1}(t) = \rho_c + \epsilon R + \epsilon^2\partial_X R \\
+ \frac{\epsilon^3}{2}\partial_X^2 R + \frac{\epsilon^4}{6}\partial_X^3 R + \frac{\epsilon^5}{24}\partial_X^4 R.
\end{aligned}
\tag{29}
$$

$$
\begin{aligned}
\rho_{j+1}(t+\tau) - 2\rho_j(t+\tau) + \rho_{j-1}(t+\tau) \\
= \epsilon^3\partial_X^2 R + \epsilon^4(b\tau)\partial_X^3 R \\
+ \frac{\epsilon^5}{12}(1+6b^2\tau^2)\partial_X^4 R.
\end{aligned}
\tag{30}
$$

The expansion of optimal velocity function at the turning point is

$$
\begin{aligned}
V(\rho_j) = V(\rho_c) + V'(\rho_c)(\rho_j - \rho_c) \\
+ \frac{V'''(\rho_c)}{6}(\rho_j - \rho_c)^3.
\end{aligned}
\tag{31}
$$

$$
\begin{aligned}
V(\rho_{j+1}) = V(\rho_c) + V'(\rho_c)(\rho_{j+1} - \rho_c) \\
+ \frac{V'''(\rho_c)}{6}(\rho_{j+1} - \rho_c)^3.
\end{aligned}
\tag{32}
$$

Using Eqs. (31) and (32), we get

$$
\begin{aligned}
V(\rho_{j+1}) - V(\rho_j) \\
= V'(\rho_c)\left[\epsilon^2\partial_X R + \frac{\epsilon^3}{2}\partial_X^2 R + \frac{\epsilon^4}{6}\partial_X^3 R + \frac{\epsilon^5}{24}\partial_X^4 R\right] \\
+ \frac{V'''(\rho_c)}{6}\left[\epsilon^4\partial_X R^3 + \frac{\epsilon^5}{2}\partial_X^2 R^3\right].
\end{aligned}
\tag{33}
$$

Some other important expansions are also computed using Eqs. (27)–(33) and are given as

$$
\begin{aligned}
V'(\rho_{j+2}(t))\tilde{\Delta}\rho_{j+2}(t) - 2V'(\rho_{j+1}(t))\tilde{\Delta}\rho_{j+1}(t) \\
+ V'(\rho_j(t))\tilde{\Delta}\rho_j(t) = \epsilon^3(b\tau)V'(\rho_c)\partial_X^2 R \\
+ \epsilon^4(b\tau)V'(\rho_c)\partial_X^3 R \\
+ \frac{\epsilon^5}{2}(b^2\tau^2 + 2b\tau)V'(\rho_c)\partial_X^4 R.
\end{aligned}
\tag{34}
$$

$$
\begin{aligned}
V(\rho_{j+2}) - 2V(\rho_{j+1}) + V(\rho_j) \\
= \epsilon^3 V'(\rho_c)\partial_X^2 R + \epsilon^4 V'(\rho_c)\partial_X^3 R \\
+ \frac{7\epsilon^5}{12}V'(\rho_c)\partial_X^4 R.
\end{aligned}
\tag{35}
$$

$$
\begin{aligned}
V'(\rho_{j+1}(t))\tilde{\Delta}\rho_{j+1}(t) - V'(\rho_j(t))\tilde{\Delta}\rho_j(t) \\
= \frac{\epsilon^3}{2}(b\tau)V'(\rho_c)\partial_X^2 R
\end{aligned}
$$

$$+ \frac{\epsilon^4}{2}(B^2\tau^2 + b\tau)V'(\rho_c)\partial_X^3 R + \epsilon^5 V'(\rho_c)$$

$$\times \left[\tau\,\partial_T\,\partial_X R + \frac{(4b\tau + 6b^2\tau^2 + 4b^3\tau^3)}{24}\partial_X^4 R\right].$$

(36)

By inserting (27), (28), (30), (33), (34), (35) and (36) into Eq. (8), we obtain Eq. (19).

References

1. Jiang, R., Wu, Q.S., Zhu, Z.J.: A new continuum model for traffic flow and numerical tests. Transp. Res. B **36**, 405–419 (2002)
2. Gupta, A.K., Katiyar, V.K.: A new anisotropic continuum model for traffic flow. Phys. A **368**, 551–559 (2006)
3. Gupta, A.K., Katiyar, V.K.: Analyses of shock waves and jams in traffic flow. J. Phys. A Math. Gen. **38**, 4069–4083 (2005)
4. Gupta, A.K., Katiyar, V.K.: Phase transition of traffic states with on-ramp. Phys. A **371**, 674–682 (2006)
5. Gupta, A.K., Redhu, P.: Analyses of the drivers anticipation effect in a new lattice hydrodynamic traffic flow model with passing. Nonlinear Dyn. **76**, 1001–1011 (2014)
6. Huang, H.J., Tang, T.Q., Gao, Z.Y.: Continuum modeling for two-lane traffic flow. Acta Mech. Sin. **22**, 131–137 (2006)
7. Tang, T.Q., Li, C.Y., Wu, Y.H., Huang, H.J.: Impact of the honk effect on the stability of traffic flow. Phys. A **390**, 3362–3368 (2011)
8. Tang, T.Q., Li, C.Y., Huang, H.J., Shang, H.Y.: A new fundamental diagram theory with the individual difference of the drivers perception ability. Nonlinear Dyn. **67**, 2255–2265 (2012)
9. Tang, T.Q., Huang, H.J., Xu, G.: A new macro model with consideration of the traffic interruption probability. Phys. A **387**, 6845–6856 (2008)
10. Tang, T.Q., Huang, H.J., Wong, S.C., Xu, X.Y.: A new overtaking model and numerical tests. Phys. A **376**, 649–657 (2007)
11. Nagatani, T.: Modified KdV equation for jamming transition in the continuum models of traffic. Phys. A **261**, 599–607 (1998)
12. Ge, H.X., Cheng, R.J.: The backward looking effect in the lattice hydrodynamic model. Phys. A **387**, 6952–6958 (2008)
13. Peng, G.H., Cai, X.H., Cao, B.F., Liu, C.Q.: Non-lane-based lattice hydrodynamic model of traffic flow considering the lateral effects of the lane width. Phys. Lett. A **375**, 2823–2827 (2011)
14. Peng, G.H., Cai, X.H., Liu, C.Q., Tuo, M.X.: A new lattice model of traffic flow with the anticipation effect of potential lane changing. Phys. Lett. A 376, 447–451 (2012)
15. Peng, G.H.: A new lattice model of traffic flow with the consideration of individual difference of anticipation driving behavior. Commun. Nonlinear Sci. Numer. Simul. **18**, 2801–2806 (2013)
16. Kang, Y.R., Sun, D.H.: Lattice hydrodynamic traffic flow model with explicit drivers physical delay. Nonlinear Dyn. **71**, 531–537 (2013)
17. Ge, H.X., Dai, S.Q., Xue, Y., Dong, L.Y.: Stabilization analysis and modified Korteweg–de Vries equation in a cooperative driving system. Phys. Rev. E **71**, 066119 (2005)
18. Ge, H.X., Ge, H.X., Cheng, R.J., Lei, L.: The Korteweg–de Vries soliton in the lattice hydrodynamic model. Phys. A **388**, 1682–1686 (2009)
19. Ge, H.X., Cheng, R.J., Lei, L.: The theoretical analysis of the lattice hydrodynamic models for traffic flow theory. Phys. A **389**, 2825–2834 (2010)
20. Li, X.L., Li, Z.P., Han, X.L., Dai, S.Q.: Effect of the optimal velocity function on traffic phase transitions in lattice hydrodynamic models. Commun. Nonlinear Sci. Numer. Simul. **14**, 2171–2177 (2009)
21. Peng, G.H., Cai, X.H., Liu, C.Q., Cao, B.F.: A new lattice model of traffic flow with the consideration of the driver's forecast effects. Phys. Lett. A **375**, 2153–2157 (2011)
22. Peng, G.H., Cai, X.H., Cao, B.F., Liu, C.Q.: A new lattice model of traffic flow with the consideration of the traffic interruption probability. Phys. A **391**, 656–663 (2012)
23. Peng, G.H., Nie, F.Y., Cao, B.F., Liu, C.Q.: A drivers memory lattice model of traffic flow and its numerical simulation. Nonlinear Dyn. **67**, 1811–1815 (2012)
24. Nagatani, T.: Jamming transitions and the modified Korteweg–de Vries equation in a two-lane traffic flow. Phys. A **265**, 297–310 (1999)
25. Nagatani, T.: Jamming transition in a two-dimensional traffic flow model. Phys. Rev. E **59**, 4857 (1999)
26. Nagatani, T.: Jamming transition of high-dimensional traffic dynamics. Phys. A **272**, 592–611 (1999)
27. Peng, G.H.: A new lattice model of two-lane traffic flow with the consideration of optimal current difference. Commun. Non. Sci. Numer. Simul. **18**, 559–566 (2013)
28. Wang, T., Gao, Z.Y., Zhao, X.M., Tian, J.F., Zhang, W.Y.: Flow difference effect in the two-lane lattice hydrodynamic model. Chin. Phys. B **21**, 070507 (2012)
29. Peng, G.H.: A new lattice model of the traffic flow with the consideration of the driver anticipation effect in a two-lane system. Nonlinear Dyn. **73**, 1035–1043 (2013)
30. Gupta, A.K., Redhu, P.: Analyses of drivers anticipation effect in sensing relative flux in a new lattice model for two-lane traffic system. Phys. A **390**, 5622–5632 (2013)
31. Zhang, M., Sun, D.H., Tian, C.: An extended two-lane traffic flow lattice model with drivers delay time. Nonlinear Dyn. **77**, 839–847 (2014)